

Negative Result

Metabotropic glutamate receptor mGluR5 is not involved in the early hemodynamic response

Novella Calcinaghi¹, Renaud Jolivet^{1,5}, Matthias T Wyss^{1,2,5}, Simon M Ametamey³, Fabrizio Gasparini⁴, Alfred Buck² and Bruno Weber¹

¹Institute of Pharmacology and Toxicology, University of Zurich, Zurich, Switzerland; ²PET Center, Division of Nuclear Medicine, University Hospital Zurich, Zurich, Switzerland; ³Center for Radiopharmaceutical Science of ETH, PSI, and USZ, Department of Chemistry and Applied Biosciences of ETH, Zurich, Switzerland; ⁴Novartis Institutes for Biomedical Research, Basel, Switzerland

Activation of astrocytic metabotropic glutamate receptor 5 (mGluR5) is postulated to elicit calcium transients, triggering a chain of events that ultimately regulates cerebral blood flow by changing the tone of smooth muscle cells of nearby arterioles. Using concurrent *in vivo* optical imaging and determination of receptor occupancy with ¹¹C-ABP688, we report here that blocking ~80% of mGluR5 *in vivo* does not affect transient hemodynamic responses on brief whisker stimulations while transiently reducing neuronal activity as measured by voltage-sensitive dye imaging. Our results show that mechanisms other than activation of mGluR5 are required to trigger the initial hemodynamic response in normal physiological conditions.

Journal of Cerebral Blood Flow & Metabolism (2011) **31**; doi:10.1038/jcbfm.2011.96; published online 6 July 2011

Keywords: astrocytes; glutamate; G-protein-coupled receptor; metabotropic glutamate receptor mGluR5; neurovascular coupling

Introduction

Neurovascular coupling (NVC) refers to the relationship between local neural activity and subsequent changes in cerebral blood flow (CBF). First described by Mosso in 1881, NVC ensures the proper supply of oxygen and nutrients to active brain regions and was subsequently shown to reflect the relaxation of vascular smooth muscle cells—and perhaps pericytes—of a specific brain area in response to a localized enhancement of neuronal activity. NVC is mediated by a complex flow of information among neurons, astrocytes, pericytes, and the vasculature, which act in concert to maintain proper cerebral perfusion.

Research in the field of NVC is highly relevant because it provides the basis for a better understanding of widely used functional imaging modalities based on CBF as a surrogate of neuronal activity.

Furthermore, many of the most severe neurodegenerative diseases involve the vascular system, as well as the supply of blood-borne substrates and oxygen. Although the complex processes governing the regulation of local CBF are not completely understood and many important questions still unanswered, astrocytes have been identified in the last few years as key players in controlling local blood flow. Strategically located in an ideal position between neurons and vessels, astrocytes can integrate neurotransmitter signals from thousands of synapses (Bushong *et al*, 2002) and relay this information to the arterioles (Metea and Newman, 2006). The specific close interactions among these different cell populations have led to the concept of a neuron–astrocyte–vasculature tripartite functional unit (Vaucher and Hamel, 1995).

One astrocytic pathway in particular has recently attracted a lot of attention. It has been reported that activation of the astrocytic metabotropic glutamate receptor mGluR5 triggers Ca²⁺ transients in astrocytes (Wang *et al*, 2006) and affects NVC (Zonta *et al*, 2003). Antagonists of group I metabotropic glutamate receptors (mGluR1 and mGluR5) were found to inhibit Ca²⁺ elevation in astrocytic endfeet and to reduce CBF increase in the somatosensory cortex of rodents on forepaw stimulation (Zonta *et al*, 2003).

Correspondence: Professor B Weber, Institute of Pharmacology and Toxicology, Department of Nuclear Medicine, University of Zurich, University Hospital Zurich, Rämistrasse 100, Zurich CH-8091, Switzerland.

E-mail: bweber@pharma.uzh.ch

⁵These authors contributed equally to this work.

Received 28 March 2011; revised 21 May 2011; accepted 31 May 2011

It is postulated that these astrocytic Ca^{2+} transients lead, in turn, to the production and release of vasoactive prostaglandin E_2 by astrocytes (Takano *et al*, 2006). The enzyme phospholipase A_2 mediates this mechanism. In the mouse olfactory bulb, the role of mGluRs in the regulation of NVC is still controversial. Gurden *et al* (2006) discarded any involvement of metabotropic receptors in intrinsic signals evoked by odors, and the local odor-evoked CBF functional increase was not affected by LY367385 application to one glomerulus (Chaigneau *et al*, 2007). However, Petzold *et al* (2008) have described a reduction of glomerular functional hyperemia on topical application of 6-methyl-2-(phenylethynyl)-pyridine (MPEP) and (5)- α -methyl-4-carboxyphenylglycine (MCPG), respectively, on selective mGluR5 and unselective group I/II mGluR antagonists.

Metabotropic glutamate receptor 5 is a G-protein-coupled receptor that has a key role in the release of Ca^{2+} from internal stores via inositol triphosphate mobilization. It is highly expressed mainly in telencephalic regions, including the cerebral cortex, hippocampus, subiculum, olfactory bulbs, and nucleus striatum (Ferraguti and Shigemoto, 2006). High levels of astrocytic mGluR5 expression have also been observed in reactive glia and are thus often associated with non-physiological conditions (Aronica *et al*, 2000; Notenboom *et al*, 2006).

Here, we report that pharmacological blockage of mGluR5 and mGluR1 does not affect NVC in the somatosensory cortex of adult anesthetized rats on brief whisker stimulation of 4 and 24 seconds. Concurrent β -probe measurements using the radiotracer ^{11}C -ABP688, which binds with high specificity to the allosteric site of mGluR5 (Wyss *et al*, 2007), show that our protocol leads to a pharmacological receptor blockage of $\sim 80\%$ in the somatosensory cortex, confirming blood–brain barrier passage and binding action of the drug. Under the same conditions, voltage-sensitive dye (VSD) imaging shows a transient reversible reduction of neuronal activity on mGluR5 blockage within the first minutes. Taken together, these results suggest that mGluR5 activation does not have a significant role in the onset and possibly in the short-term maintenance of the hemodynamic response in adult rats, and thus call for a revision of the current astrocytic model of NVC at these time scales.

Materials and methods

Animals

The experiments were performed by licensed investigators, and the experimental procedures were reviewed by an ethical committee and authorized by the cantonal veterinary authority. They conform to the guidelines of the Swiss Animal Protection Law, Veterinary Office, Canton Zurich (Act of Animal Protection 16 December 2005 and Animal Protection Ordinance 23 April 2008).

The animals (40 male Sprague–Dawley rats weighing 200 to 300 g) were provided by Harlan Laboratories (Horst, Netherlands) and were kept in cages in a ventilated cabinet with standardized conditions of light (night/day cycle: 12 hour/12 hour) and temperature, and free access to food and water was permitted. To exclude a strain effect, additional experiments were conducted using Wistar rats ($n=3$); no difference was observed between the two strains (data not shown).

Surgical Preparation

All surgical procedures were performed under isoflurane anesthesia (2.5% to 3.5%). Catheters (PE-50) were inserted into the right femoral artery and vein. For radiotracer measurements, the vessels of the left hindlimb were also cannulated for the placement of an arteriovenous shunt. The animals were tracheotomized and artificially ventilated. The skull above the barrel cortex (1 mm caudal and 3 to 6 mm lateral from bregma) was carefully thinned using a dental drill (Bien Air Medical Technologies, Bienne, Switzerland). The thinned area was then covered with 2% agarose type III-A (Sigma, St Louis, MO, USA) in Ringer's solution (in g/L: NaCl 8.6, CaCl_2 0.30, and KCl 0.30) and with a circular glass coverslip of 5-mm diameter. The animals' temperature was kept at 37°C with a heating blanket and blood gases were maintained within physiological ranges by adjusting the ventilation when necessary. After surgery, isoflurane was discontinued (or reduced to a maximum of 0.5% when necessary) and anesthesia was maintained with a first subcutaneous injection of α -chloralose (44 mg/kg; Sigma, Buchs, Switzerland), followed by continuous subcutaneous infusion (22 mg/kg/hour). This anesthetic regime is considered ideal for studies of neurovascular and neurometabolic coupling (Bonvento *et al*, 1994). The level of anesthesia was controlled by observing arterial blood pressure during stimulation and by tail pinch. Experiments were performed after a postoperative recovery period of at least 1 hour to obtain a stable level of α -chloralose anesthesia and stable imaging signals.

Sensory Stimulation

After a baseline of 2 seconds, the vibrissae contralateral to the thinned skull were deflected using air puffs for 4 seconds at a frequency of 4 Hz. Ten trials were averaged for each subexperiment. In an additional subset of experiments, after a baseline of 4 seconds, vibrissae were deflected for 24 seconds and five trials were averaged for each recording. For VSD experiments, a single whisker was deflected once and 10 trials were averaged for each condition.

Intrinsic Optical Imaging

Cortical images were acquired using two 12-bit CCD cameras (Pixelfly VGA, PCO Imaging, Kelheim, Germany) attached to a motorized epifluorescence stereomicroscope (Leica MZ16 FA, Leica Microsystems, Heerbrugg, Switzerland) focused 0.5 mm below the cortical surface.

Two-dimensional optical spectroscopy was performed using the method described by Dunn *et al* (2003). The six wavelengths (560, 570, 580, 590, 600 and 610 nm, 10 nm full width at half maximum (FWHM)) were produced with a monochromator (Polychrome V, Till Photonics, Grafelfing, Germany) and coupled in the microscope using an optical fiber. Images were acquired with 30 Hz and the monochromator was synchronized with the image acquisition (each frame was acquired with a different illumination wavelength). The second camera was used to simultaneously measure CBF using dynamic laser speckle imaging. The method is described in detail elsewhere (Zakharov *et al*, 2009). A 785-nm laser light (TuiOptics, Munich, Germany) was shone onto the cortex and images were acquired at 30 Hz with an exposure time of 10 milliseconds.

Pharmacological Interventions

6-Methyl-2-(phenylethynyl)-pyridine and LY367385 were supplied by Tocris Bioscience (Bristol, UK) and injected intravenously at 1.2 mg/kg body weight or 4.0 mg/kg as specified in the text (dissolved in dimethyl sulfoxide, dimethyl sulfoxide reaching a maximum of 2% of the final concentration in NaCl). 6-Cyano-7-nitroquinoline-2,3-dione (Tocris Bioscience) was injected at 15 mg/kg body weight (1:1 polyethylene glycol:NaCl). 2-(3-Methoxy-phenylethynyl)-6-methyl-pyridine (M-MPEP), provided by FG, was administered intravenously at different concentrations (in a range from 1 to 8 mg/kg, as specified in the text; 1:1 polyethylene glycol:NaCl). Both the MPEP and M-MPEP infusions were delivered at a very slow rate (~ 0.2 mL/minute).

Radiotracer Experiments

^{11}C -ABP688, a PET ligand for the study of mGluR5 (Wyss *et al*, 2007), was used for the determination of receptor density (B_{max}) before and 10 minutes after injection of M-MPEP. Radiotracer experiments included measurements of time courses of tracer accumulation in the left somatosensory cortex using a beta scintillator for surface acquisitions (Wyss *et al*, 2009) and the online acquisition of total arterial ^{11}C activity in the arteriovenous shunt. For the latter purpose, the shunt was run through a coincidence counter (GE Medical Systems, Opfikon, Switzerland). The online arterial sampling procedure is described in detail elsewhere (Weber *et al*, 2002). Whole-blood activity was then corrected for (i) the relative concentration of ^{11}C -ABP688 in plasma versus whole blood and (ii) the concentration of labeled metabolites.

For the tissue acquisitions, the scintillator was adjusted just above the thinned skull covering the somatosensory cortex. The count rate was stored on a personal computer using a bin width of 1 second, yielding tissue time-activity curves. During both conditions (baseline/blockage), data were acquired for 20 minutes. After each experiment, the beta scintillator was calibrated with a known concentration of ^{11}C activity. Injected activities were in the range of 40 to 104 MBq throughout all experiments, and the injected mass of ABP688 was 0.49 to 4.08 pmoles/g body weight. This methodology used to quantify mGluR5 using ^{11}C -ABP688 is described in detail elsewhere (Wyss *et al*, 2007).

Voltage-Sensitive Dye Imaging

For VSD imaging, the dye RH1691 was dissolved at 1 mL/mL in Ringer's solution. A cranial window was drilled on the right hemisphere above the whisker barrel cortex (bregma, 0 to -5 mm; lateral, 2 to 7 mm). After removal of the bone, dura was left intact to reduce movement artifact and tendency to edema. Around the craniotomy, a few layers of dental cement were applied to form a trough to prevent dye leakage during the staining process. The dye was topically applied and was allowed to diffuse into the cortex for 90 minutes. During staining, the dye was continuously circulated by a peristaltic pump (Reglo digital, Ismatec SA, Glattbrugg, Switzerland). Thereafter, the unbound dye was removed and the area was washed with dye-free Ringer's solution for more than 15 minutes. The fluid-filled chamber was then covered with a glass coverslip. For imaging, the dye was excited with 630-nm light from a LED lamp (Thorlabs GmbH, Dachau/Munich, Germany). The excitation light was reflected by a 650-nm dichroic mirror and focused onto the cortical surface with a camera lens. Fluorescent emission light was collected via the same optical pathway, but without mirror reflection, long-pass filtered (>670 nm), and focused onto the sensor of a high-speed Micam Ultima camera (Scimedia, Costa Mesa, CA, USA). This high-speed CMOS-based camera has a detector of $100 \times 100 \mu\text{m}$. Images were collected with 1-millisecond temporal resolution. Acquisitions were performed before and 5, 15, 30, 45, and 60 minutes after the intravenous injection of 4 mg/kg M-MPEP. Because of the high sensitivity of the VSD method, the VSD signal was elicited by a single whisker deflection.

Data Analysis

Image analysis and radiotracer kinetic analysis were performed using custom-written Matlab routines and the software package PMOD (Mikolajczyk *et al*, 1998).

Optical Imaging: The analysis of the multiwavelength spectroscopy followed the protocol of Dunn *et al* (2003). Baseline values for total hemoglobin concentrations were set to $100 \mu\text{moles/L}$ with 70% oxygen saturation, which implies $C_0^{\text{HbO}} = 70 \mu\text{moles/L}$ and $C_0^{\text{HbR}} = 30 \mu\text{moles/L}$. To quantify CBF, speckle images were processed as described recently (Zakharov *et al*, 2009) using 5×5 spatial and 25 temporal binning. Circular regions of interest (0.5 mm^2) were drawn manually over the area of maximal signal increase to extract the signal time courses. The 10 trials (5 in long-term stimulation experiments), which were performed within 12 minutes in each animal, were averaged. All data represent the mean \pm s.e.m. used for each experimental condition. Spectroscopic and CBF maximum signals in the presence of pharmacological intervention were normalized to the control condition.

^{11}C -ABP688 Radiotracer Kinetic Modeling: The applied methods consisted of standard compartmental modeling using an arterial input function. Tracer kinetics were modeled using a two-tissue compartment model with rate constants K_1 – k_4 , which has been shown to be suitable for

the description of ^{11}C -ABP688 data (Wyss *et al*, 2007). To achieve stable fits, K_1/k_2 and k_4 were fixed at 1.6 and 0.05/minute, respectively, for both conditions (baseline/blockage), corresponding to mean values of free fitting using two tissue compartments. For data analysis, background counts were subtracted and all time–activity curves were decay corrected (physical half-life = 20.38 minutes) to the time point of injection and converted to kBq/mL taking into account a determined calibration factor (see above). For details of the analysis procedure, see the previous description of the approach (Wyss *et al*, 2007).

Voltage-Sensitive Dye: Bleaching of fluorescence was corrected by subtraction of a best-fit double exponential. Time courses of fluorescence changes were quantified as $\Delta F/F_0$ from circular regions of interest of constant diameter adjusted to the activation area. To compare VSD signals from different animals, regions of interest were centered on the location of the earliest response. Amplitude was defined as the difference between the maximal response and the baseline signal just before the onset of whisker stimulation. Within single studies, amplitude changes across acquisitions were normalized to the signal amplitude of the baseline examination (=acquisition before M-MPEP injection).

Statistics: The required sample size was estimated before the study based on published data (Zonta *et al*, 2003), where a CBF response of $23 \pm 7.0\%$ (mean \pm s.e.m.; $n=5$) was reduced to $8 \pm 1.8\%$ by mGluR blockage. The authors report that a *t*-test for paired samples yielded $P < 0.01$, from which follows $t \geq 4.6$ ($df=4$) and effect size $d \geq 2.05$. On the basis of these parameters, a minimum sample size of $n=8$ was determined (Software G*power, University of Düsseldorf, Germany). Differences between hemodynamic responses before and after receptor blockage were statistically analyzed using the Wilcoxon signed-rank test.

Results

To control for the role of mGluR5 in the regulation of CBF, we assessed NVC before and after pharmacological manipulations of the receptor. More specifically, we used multiwavelength spectroscopy to reveal quantitative spatio-temporal changes of deoxyhemoglobin (HbR), oxyhemoglobin (HbO), and total hemoglobin (HbT) concentrations. Concurrently, we used laser speckle contrast imaging maps to measure relative CBF changes (Zakharov *et al*, 2009).

Transient Hemodynamic Responses of the Somatosensory Cortex Are Not Affected by Metabotropic Glutamate Receptor 5 Blockage

Figure 1A shows a typical hemodynamic response of the somatosensory cortex on brief whisker stimulation with colocalized changes in HbR, HbO, HbT and CBF. Spatio-temporal hemodynamic and metabolic responses were measured in a series of (i) control experiments ($n=5$ animals) and in the absence and presence of pharmacological intervention using (ii) MPEP and LY367385 ($n=7$ animals),

(iii) M-MPEP ($n=8$ animals), and (iv) 6-cyano-7-nitroquinoxaline-2,3-dione ($n=6$ animals). To investigate the effect of group I mGluR block on NVC, MPEP and LY367385 (mGluR5 and mGluR1 blockers, respectively) were administered intravenously (1.2 mg/kg). These compounds readily pass through the blood–brain barrier (Gasparini *et al*, 1999, 2002). Surprisingly, no significant changes were observed in the evoked hemodynamic responses after blockage of these mGluRs (Figure 1B and 1C). To further confirm these results, we studied the effect of a more effective mGluR5 blocker, M-MPEP, which is five times more potent than MPEP (Gasparini *et al*, 1999, 2002). Again, no significant reduction of evoked hemodynamic signals was observed between baseline condition and 10 minutes after M-MPEP pharmacological intervention (Figures 1B and 1C). However, the CBF signal was slightly but significantly increased by M-MPEP injection. In a separate set of animals, hemodynamic responses were evaluated before and 10 minutes after systemic injection of 6-cyano-7-nitroquinoxaline-2,3-dione (CNQX), an AMPA/kainate receptor antagonist. The neuronal activity block elicited a significant reduction in all hemodynamic parameters and in CBF.

Steady-State Hemodynamic Responses Are Not Affected by Blockage of Group I Metabotropic Glutamate Receptors

After demonstrating that group I mGluR block does not affect NVC mechanisms during brief whisker stimulation, we wanted to explore the contribution of mGluR5 to more sustained blood flow responses. Hemodynamic responses before and after injection of group I mGluR antagonists were evaluated in four animals during 24 seconds of whisker stimulation. Stimulus-evoked responses exhibited an initial peak, followed by a steady-state component that lasted until the stimulation was discontinued (Figure 2A). Similar responses have been previously reported (Berwick *et al*, 2008). Both the initial peak and the steady-state component did not exhibit any change after MPEP and LY367385 intravenous injection (4.0 mg/kg) as reported in CBF example curves (Figure 2A). On the contrary, a brief systemic increase in mean arterial blood pressure was recorded (significantly different only during the first 5 minutes after systemic injection; $P < 0.05$, Figure 2B), which was not observed during placebo experiments (same volume of 1:1 polyethylene glycol:NaCl; data not shown).

Intravenous Injection of Metabotropic Glutamate Receptor 5 Antagonists Leads to High Levels of Receptor Occupancy

Next, we verified that the administration of MPEP and M-MPEP did indeed significantly block mGluR5 in our protocol. To this end, we conducted a series of concurrent optical/radiotracer experiments to quantify cortical mGluR5 occupancy and its effect on the hemodynamic response ($n=5$). Using ^{11}C -ABP688, both MPEP and M-MPEP were found to significantly reduce radiolabel binding to the tissue

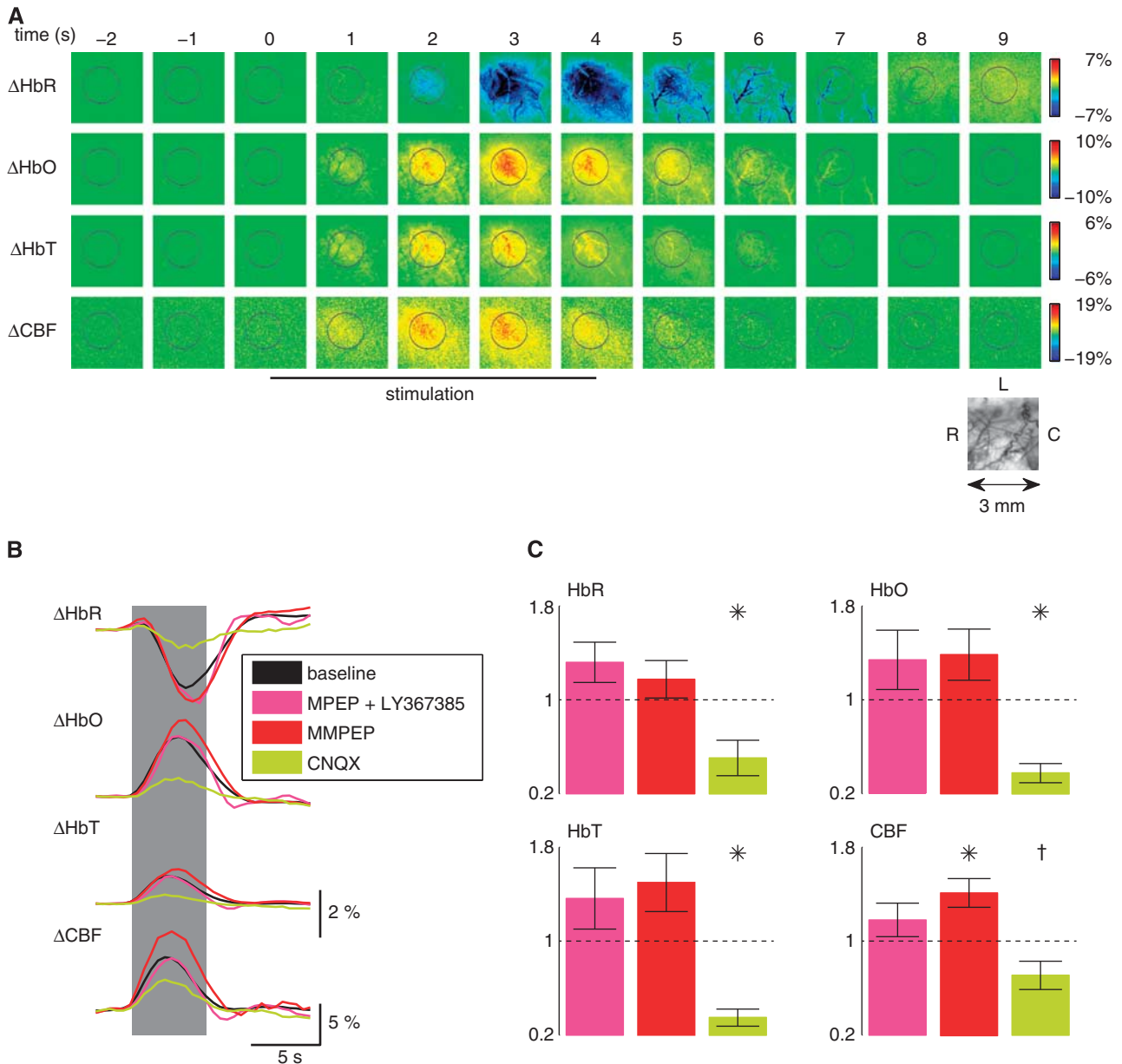


Figure 1 Application of group I metabotropic glutamate receptor (mGluR) antagonists does not affect neurovascular coupling on brief whisker stimulation. **(A)** Relative changes of deoxy- (HbR), oxyhemoglobin (HbO), and blood volume (HbT) on brief whisker stimulation were measured by optical spectroscopy in the activated barrel cortex, whereas cerebral blood flow (CBF) was measured by laser speckle imaging. **(B)** Average responses after intravenous injection of the mGluR5 and mGluR1 antagonists 6-methyl-2-(phenylethynyl)-pyridine (MPEP) and LY367385, respectively (1.2 mg/kg; pink), and after injection of 2-(3-methoxy-phenylethynyl)-6-methyl-pyridine (M-MPEP; four animals at 1 mg/kg; one animal at 2 mg/kg; one animal at 3 mg/kg; and two animals at 4 mg/kg; red) compared with baseline (black). Data shown were recorded 10 minutes after drug injection. No significant decrease of the response was observed after these treatments (statistical testing either for the MPEP-LY367385 and M-MPEP groups separately or for the two groups pooled together, $n = 15$). In contrast, after treatment with 6-cyano-7-nitroquinoxaline-2,3-dione (CNQX; 15 mg/kg; green; $n = 6$), a strong reduction in the hemodynamic signals was evident. **(C)** Peak deviations normalized to baseline (mean \pm s.e.m.; * $P < 0.05$, † $P = 0.075$, Wilcoxon signed-rank test). In total, MPEP-LY367385, M-MPEP, and CNQX were tested, respectively, in 7, 8, and 6 rats. Measurements at the later time points (30 and 45 minutes) did not show any significant decrease of the peak response (data not shown).

compared with baseline condition, without having a noticeable effect on the hemodynamic response (Figure 3). Radiotracer activity was recorded for a period of 20 minutes,

beginning 10 minutes after MPEP or M-MPEP injection. On average, a 57% reduction in the density of free receptors in the tissue was measured (B_{max} ; Figure 3D).

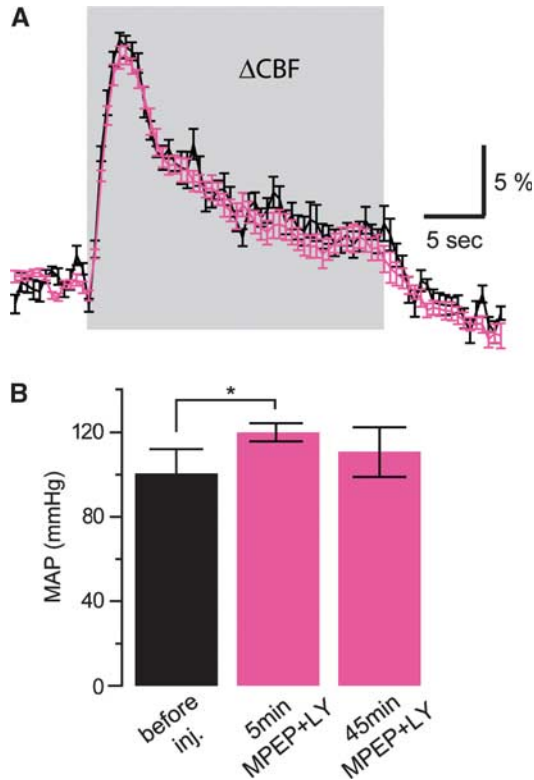


Figure 2 The neurovascular coupling response during longer stimulation is also not affected by group I metabotropic glutamate receptor antagonists 6-methyl-2-(phenylethynyl)pyridine (MPEP) and LY367385. **(A)** Example of cerebral blood flow (CBF) recordings during 24-second whisker stimulation before (black) and 10 minutes after (pink) MPEP and LY367385 intravenous injection (4.0 mg/kg). **(B)** Systemic effect on mean arterial blood pressure (MAP) evoked by MPEP and LY367385 intravenous injection (4.0 mg/kg). Five minutes after drug injection, a significant increase was observed (MAP before injection: 101 ± 11 mm Hg; 5 minutes after injection: 120 ± 4 mm Hg; 45 minutes after injection: 111 ± 11 mm Hg; mean \pm s.d.; $n = 4$; $*P < 0.05$, Wilcoxon signed-rank test) before the arterial blood pressure returned to its baseline. This transient increase was not elicited by placebo injection (see text).

Evoked Neuronal Activity in the Somatosensory Cortex is Transiently Reduced by Metabotropic Glutamate Receptor 5 Blockage

To assess the potential impact of mGluR5 blockage on neuronal activity, and, in particular, to control for changes in the spatiotemporal dynamics of cortical brain activity on mGluR5 blockage by M-MPEP, VSD experiments were performed. VSD imaging provides a visualization of the cortical activity of a large neuronal population in the upper cortical layers with high spatial and temporal resolution (Chemla and Chavane, 2010). VSD fluorescent signals evoked by a single whisker deflection were recorded in control conditions and after M-MPEP intravenous injection (4 mg/kg, $n = 6$). The VSD signal was slightly decreased, on average by 27% 5 minutes after M-MPEP injection

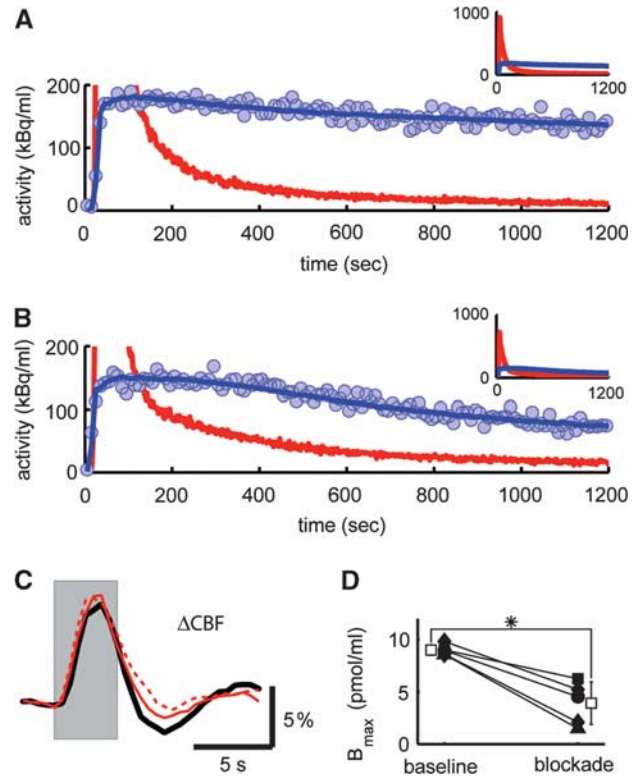


Figure 3 Delivery of 2-(3-methoxy-phenylethynyl)-6-methylpyridine (M-MPEP) leads to blockage of metabotropic glutamate receptor 5 (mGluR5) in the rat somatosensory cortex but fails to attenuate the hemodynamic response. After the injection of M-MPEP (4 mg/kg), the washout of radiolabel from tissue was increased **(B)** compared with baseline condition **(A)** as represented by the decay-corrected tissue time-activity curves (blue circles). The model curve (blue line) and the radioactivity concentration in plasma (that is input curve; red line) are also shown. In **A** and **B**, the ordinate is truncated at 200 kBq/mL for legibility reasons. The full range of data is displayed in the insets (same axes legends). In this example, the estimated mGluR5 blockage amounted to 47%. **(C)** Hemodynamic response on stimulation (gray area) before (black line), 10 minutes (red line), and 30 minutes (broken red line) after delivery of M-MPEP (same experiment as in **A** and **B**) was unaffected by mGluR5 blockage. **(D)** The density of receptors in the tissue (B_{max}) is shown for all individual β -probe experiments before and after blockade (square: 1.2 mg/kg 6-methyl-2-(phenylethynyl)pyridine/LY367385; circle: 1 mg/kg M-MPEP; diamond: 4 mg/kg M-MPEP; and triangle: 8 mg/kg M-MPEP). White boxes represent mean \pm s.d. ($*P < 0.05$, Wilcoxon signed-rank test).

(Figure 4). Measurements at later time points revealed this effect to be completely reversible, indicating a transient reduction in neuronal activity in response to mGluR5 block.

Discussion

Recent years have seen a surge in research on the physiology of astrocytes, and the regulation of local

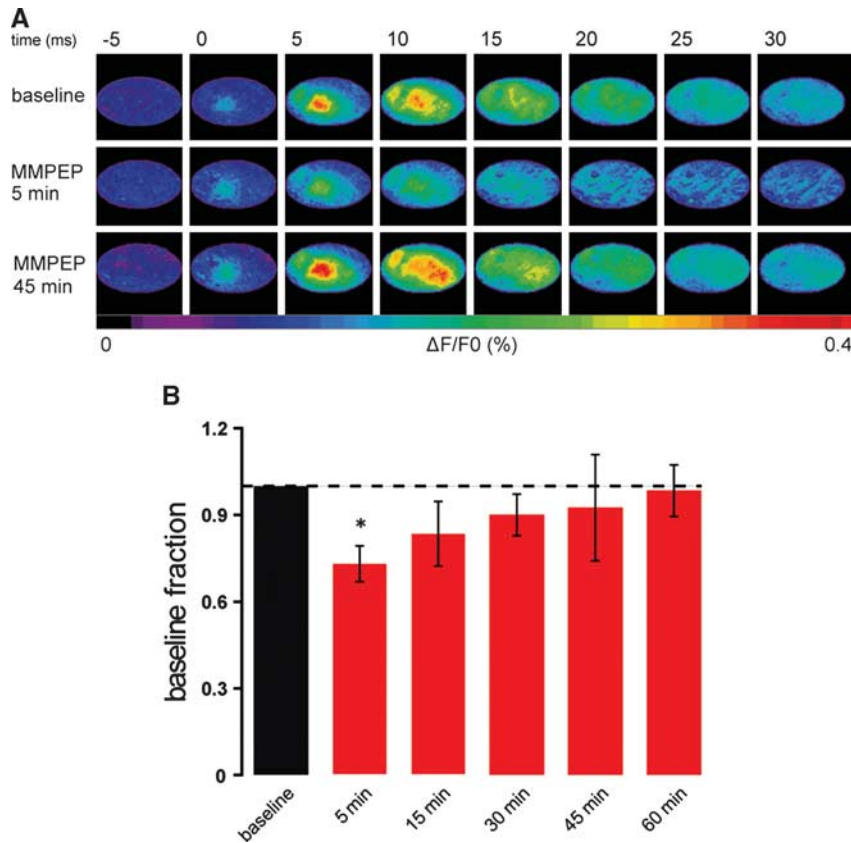


Figure 4 Neuronal activity slightly decreases during the first 30 minutes after metabotropic glutamate receptor 5 blockage. **(A)** Maps of a single voltage-sensitive dye (VSD) imaging experiment performed before (top), 5 minutes (middle), and 45 minutes (bottom) after injection of 2-(3-methoxy-phenylethynyl)-6-methyl-pyridine (M-MPEP; 4 mg/kg). Single frames are 5 milliseconds apart from each other. The series starts 5 milliseconds before single whisker stimulation evoked at time 0. **(B)** Summary of VSD results in six animals. After only 5 minutes after the injection of M-MPEP (4 mg/kg), the amplitude of the VSD signal significantly decreased by, on average, 27%. At later time points, the signal was not significantly different from baseline level; * $P < 0.05$, Wilcoxon signed-rank test.

CBF is one of the areas where a relatively comprehensive model involving astrocytes has been suggested (Attwell *et al*, 2010). This model proposes that the activation of astrocytic metabotropic glutamate receptor mGluR5 by neuronal activity triggers intracellular Ca^{2+} transients, leading to the activation of phospholipase A_2 . Phospholipase A_2 , in turn, activates a variety of pathways that ultimately lead to the release of possibly multiple vasoactive agents by astrocytes. The work presented here contradicts this model. More specifically, it contradicts the involvement of mGluR5 in triggering this complex chain of events. We have reported here that although antagonists of mGluR5 delivered intravenously cross the blood–brain barrier and block $\sim 80\%$ of the receptors (Figure 3), they fail to induce a reduction of the hemodynamic response on brief 4- and 24-second whisker stimulation (Figures 1 and 2). However, it was found that mGluR5 antagonists provoke a transient increase in mean arterial blood pressure (Figure 2) and a transient reduction of neuronal activity (Figure 4). Additionally, injection of mGluR5 antagonists did not significantly affect the baseline

CBF, which could have interacted with the hemodynamic response after the stimulation (data not shown).

As mentioned above, several studies have reported a reduction of the hemodynamic response on blockage of mGluR5 (Petzold *et al*, 2008; Takano *et al*, 2006; Zonta *et al*, 2003). Activation of mGluR5 has also been reported to elicit Ca^{2+} transients in astrocytes (Wang *et al*, 2006). The present study differs from these studies in three ways. First, we used relatively brief whisker stimulations (4 and 24 seconds), whereas a 60-second stimulation was normally applied in these studies. Secondly, we used a thinned skull preparation to keep the system as intact and healthy as possible. Finally, we used a combination of intrinsic optical imaging and laser speckle imaging, whereas in the earlier studies CBF was measured with a laser Doppler probe. This last point, however, should not affect the results. Despite the fact that laser speckle imaging maps CBF in two dimensions and laser Doppler flowmetry is normally a point measurement, both techniques essentially rely on the same physical principles.

It is important to note that we probed the system in a time frame comparable to the one used in other studies. For example, Zonta *et al* (2003) measured the effect of MPEP injection on CBF 15 to 20 minutes after injection. Our results show a very significant receptor occupancy 10 to 30 minutes after MPEP or M-MPEP injection (Figure 3), yet with no reduction in the hemodynamic response. In principle, the transient decrease in neural activity reflected by the decrease in VSD signal amplitude (Figure 4) should lead to a detectable reduction of the hemodynamic signal in the first few minutes after injection. One possible explanation of the absence of a hemodynamic effect is an interaction with the observed transient increase in systemic arterial blood pressure. A limitation of the present study is the fact that the stimulation protocols used for the VSD and hemodynamic imaging were not identical. Further investigation of this phenomenon will require a simultaneous acquisition of both signals to detect possible interactions on the single-trial level.

Blockage of mGluR5 by injection of the potent M-MPEP slightly but significantly increased the evoked CBF response (Figure 1C). It is difficult to give a simple explanation for this result as mGluR5 has a role in a variety of physiological processes, some of them of systemic nature, as reflected by the transiently elevated blood pressure.

Part, but not all, of the apparent contradiction between our data and previous reports could be explained by regional differences in the expression pattern of mGluR5, for example, the study by Petzold *et al* (2008) focused on the olfactory bulb. However, the question remains open whether astrocytic mGluR5 has a role in NVC. We note that the literature does not unequivocally support a key physiological role for astrocytic mGluR5 in functional hyperemia. The arguments are as follows.

First, it appears that expression of mGluR5 is mostly neuronal but that it can also be highly expressed in reactive glia. mGluR5 immunoreactivity has been reported in neurons, axons, or vesicles (Jia *et al*, 1999), and the receptor is indeed widely expressed by neurons in adult rodents (Ferraguti and Shigemoto, 2006). In support of these results, knocking out mGluR5 only in cortical excitatory neurons strongly reduces its overall expression level in the cortex (Ballester-Rosado *et al*, 2010). Moreover, in the cerebral cortex, all non-neuronal cells were found to be negative for mGluR5 by Mudo *et al* (2007). Although mGluR5 has been reported in hypothalamic (Van Den Pol *et al*, 1995) and cultured (Biber *et al*, 1999) astrocytes, high levels of astrocytic mGluR5 expression have been observed in reactive glia and are thus often associated with non-physiological conditions (Aronica *et al*, 2000; Notenboom *et al*, 2006). Consistent with this view, mGluR5 expression is increased *in vitro* in the presence of growth factors, such as transforming growth factor- α and epidermal growth factor, in the extracellular environment (Miller *et al*, 1995).

Secondly, G-protein-coupled receptors are, in general, responsible for slow postsynaptic signaling. In a recent review, Cauli and Hamel (2010) discuss the temporal sequence of astrocytic and neuronal contributions to CBF control. In both neurons and astrocytes, intracellular Ca^{2+} increases code neuronal activity and elicit several cascades of events. Neurons express ionotropic receptors more frequently and abundantly than astrocytes and consequently are able to evoke quick changes in membrane potential, inducing rapid intracellular Ca^{2+} increases in a time window of ~ 10 to 12 milliseconds. On the contrary, because of their signal transduction pathways, metabotropic receptors, in general, elicit responses of slower onset and longer duration, from seconds to potentially hours, although G-protein-coupled receptor-mediated synaptic responses can occur at relatively fast time scales of 1 to 2 seconds on strong stimulation (Chrupka and Gahwiler, 1991). Although these faster responses are compatible with functional hyperemia, it seems more likely that group I mGluRs expressed in either neurons and/or astrocytes are responsible for the slow components of Ca^{2+} dynamics (Cauli and Hamel, 2010). In different *in vivo* studies (Devor *et al*, 2008; Takano *et al*, 2006; Weber *et al*, 2004) and in the data reported here, a hemodynamic delay of ~ 500 milliseconds was observed, indicating that the transient phase of the hemodynamic response, if it is Ca^{2+} induced, is likely to be initiated by cells with fast Ca^{2+} dynamics. Astrocytes, which only in a small portion exhibit Ca^{2+} responses as fast as in neurons (Winship *et al*, 2007), potentially contribute to NVC regulation only in the later response phase.

Finally, other groups have also reported findings contradicting the mGluR5 astrocytic model. Takata and Hirase (2008) have reported that astrocytic spontaneous Ca^{2+} surges are not affected by MPEP systemic injection or pyridoxal phosphate-6-azophenyl-2',4'-disulfonic acid (a non-selective P2 purinergic antagonist) topical application in L1 and L2/3 of the somatosensory cortex of anesthetized rats (Takata and Hirase, 2008), indicating that the spontaneous astrocytic Ca^{2+} surges are independent of metabotropic glutamate or purinergic receptors. More recently, Devor's group reported that astrocytic Ca^{2+} increases are infrequent and delayed compared with the onset of vasodilation on a variety of stimulation types in the rat or mouse somatosensory cortex (Nizar *et al*, 2010). Taken together, these studies are not supportive of a predominant role for astrocytic mGluR5 in triggering the fast initial hemodynamic response and do not support the notion that the transient neurovascular response is mediated through a Ca^{2+} -related mechanism. However, our results and the literature cited above do not rule out a possible involvement of mGluR5 in the late maintenance phases of the hemodynamic response, which would then explain why other groups have observed a reduction of the neurovascular response on MPEP

delivery after longer periods of stimulation (30 to 60 seconds). However, at least for the whisker-to-barrel system, such long-lasting activity patterns are rather artificial, and rapid neuronal adaptation already occurs after a few seconds after stimulation onset.

The results presented here strongly suggest that mGluR5 does not play a crucial role in the transient phase of the hemodynamic response. Thus, the exact mechanism by which astrocytes sense the extracellular glutamate concentration and trigger intracellular events for regulation of the vascular response remains unclear, and research on this topic must be continued.

Acknowledgements

The authors acknowledge support from the Swiss National Science Foundation (Grant PP00B-110751/1 and 31003A_124739/1 to BW and MTW). RJ is supported by grants from the Olga Mayenfisch, the Hartmann Müller, and the EMDO foundations.

Disclosure/conflict of interest

The authors declare no conflict of interest. FG is an employee of Novartis Pharma AG.

References

- Aronica E, van Vliet EA, Mayboroda OA, Troost D, da Silva FH, Gorter JA (2000) Upregulation of metabotropic glutamate receptor subtype mGluR3 and mGluR5 in reactive astrocytes in a rat model of mesial temporal lobe epilepsy. *Eur J Neurosci* 12:2333–44
- Attwell D, Buchan AM, Charpak S, Lauritzen M, MacVicar BA, Newman EA (2010) Glial and neuronal control of brain blood flow. *Nature* 468:232–43
- Ballester-Rosado CJ, Albright MJ, Wu CS, Liao CC, Zhu J, Xu J, Lee LJ, Lu HC (2010) mGluR5 in cortical excitatory neurons exerts both cell-autonomous and -nonautonomous influences on cortical somatosensory circuit formation. *J Neurosci* 30:16896–909
- Berwick J, Johnston D, Jones M, Martindale J, Martin C, Kennerley AJ, Redgrave P, Mayhew JEW (2008) Fine detail of neurovascular coupling revealed by spatiotemporal analysis of the hemodynamic response to single whisker stimulation in rat barrel cortex. *J Neurophysiol* 99:787–98
- Biber K, Laurie DJ, Berthele A, Sommer B, Tolle TR, Gebicke-Harter PJ, van Calker D, Boddeke HWGM (1999) Expression and signaling of group I metabotropic glutamate receptors in astrocytes and microglia. *J Neurochem* 72:1671–80
- Bonvento G, Charbonne R, Correze JL, Borredon J, Seylaz J, Lacombe P (1994) Is alpha-chloralose plus halothane induction a suitable anesthetic regimen for cerebrovascular research. *Brain Res* 665:213–21
- Bushong EA, Martone ME, Jones YZ, Ellisman MH (2002) Protoplasmic astrocytes in CA1 stratum radiatum occupy separate anatomical domains. *J Neurosci* 22:183–92
- Cauli B, Hamel E (2010) Revisiting the role of neurons in neurovascular coupling. *Front Neuroenergetics* 2:9
- Chaigneau E, Tiret P, Lecoq J, Ducros M, Knopfel T, Charpak S (2007) The relationship between blood flow and neuronal activity in the rodent olfactory bulb. *J Neurosci* 27:6452–60
- Charpak S, Gahwiler BH (1991) Glutamate mediates a slow synaptic response in hippocampal slice cultures. *Proc Biol Sci* 243:221–6
- Chemla S, Chavane F (2010) Voltage-sensitive dye imaging: technique review and models. *J Physiol Paris* 104:40–50
- Devor A, Hillman EM, Tian P, Waeber C, Teng IC, Ruvinskaya L, Shalinsky MH, Zhu H, Haslinger RH, Narayanan SN, Ulbert I, Dunn AK, Lo EH, Rosen BR, Dale AM, Kleinfeld D, Boas DA (2008) Stimulus-induced changes in blood flow and 2-deoxyglucose uptake dissociate in ipsilateral somatosensory cortex. *J Neurosci* 28:14347–57
- Dunn AK, Devor A, Bolay H, Andermann ML, Moskowitz MA, Dale AM, Boas DA (2003) Simultaneous imaging of total cerebral hemoglobin concentration, oxygenation, and blood flow during functional activation. *Opt Lett* 28:28–30
- Ferraguti F, Shigemoto R (2006) Metabotropic glutamate receptors. *Cell Tissue Res* 326:483–504
- Gasparini F, Andres H, Flor PJ, Heinrich M, Inderbitzin W, Lingenhohl K, Muller H, Munk VC, Omilusik K, Stierlin C, Stoehr N, Vranesic I, Kuhn R (2002) [(3)H]-M-MPEP, a potent, subtype-selective radioligand for the metabotropic glutamate receptor subtype 5. *Bioorg Med Chem Lett* 12:407–9
- Gasparini F, Lingenhöhl K, Stoehr N, Flor PJ, Heinrich M, Vranesic I, Biollaz M, Allgeier H, Heckendorn R, Urwyler S, Varney MA, Johnson EC, Hess SD, Rao SP, Saccaan AI, Santori EM, Velicelebi G, Kuhn R (1999) 2-Methyl-6-(phenylethynyl)-pyridine (MPEP), a potent, selective and systemically active mGlu5 receptor antagonist. *Neuropharmacology* 38:1493–503
- Guelden H, Uchida N, Mainen Z (2006) Sensory-evoked intrinsic optical signals in the olfactory bulb are coupled to glutamate release and uptake. *Neuron* 52:335–45
- Jia H, Rustioni A, Valtschanoff JG (1999) Metabotropic glutamate receptors in superficial laminae of the rat dorsal horn. *J Comp Neurol* 410:627–42
- Metaea MR, Newman EA (2006) Glial cells dilate and constrict blood vessels: a mechanism of neurovascular coupling. *J Neurosci* 26:2862–70
- Mikolajczyk K, Szabatin M, Rudnicki P, Grodzki M, Burger C (1998) A JAVA environment for medical image data analysis: Initial application for brain PET quantitation. *Med Inform* 23:207–14
- Miller S, Romano C, Cotman CW (1995) Growth-factor up-regulation of a phosphoinositide-coupled metabotropic glutamate-receptor in cortical astrocytes. *J Neurosci* 15:6103–9
- Mosso A (1881) *Ueber den Kreislauf des Blutes im Menschlichen Gehirn*. Leipzig: Verlag von Veit & Comp
- Mudo G, Trovato-Salinaro A, Caniglia G, Cheng QZ, Condorelli DF (2007) Cellular localization of mGluR3 and mGluR5 mRNAs in normal and injured rat brain. *Brain Res* 1149:1–13
- Nizar KW, Reznichenko L, Cheng Q, Sakadzic S, Boas DA, Masliah E, Dale AM, Silva GA, Devor A (2010) Unreliable and delayed astrocytic calcium response does not support the hypothesis of calcium-dependent

- astrocytic regulation of blood flow. In: *Program No. 192.9/FFF13. 2010 Neuroscience Meeting Planner* (Planner NM, ed.), San Diego, CA: Society for Neuroscience (online)
- Notenboom RG, Hampson DR, Jansen GH, van Rijen PC, van Veelen CW, van Nieuwenhuizen O, de Graan PN (2006) Up-regulation of hippocampal metabotropic glutamate receptor 5 in temporal lobe epilepsy patients. *Brain* 129:96–107
- Petzold GC, Albeanu DF, Sato TF, Murthy VN (2008) Coupling of neural activity to blood flow in olfactory glomeruli is mediated by astrocytic pathways. *Neuron* 58:897–910
- Takano T, Tian GF, Peng WG, Lou NH, Libionka W, Han XN, Nedergaard M (2006) Astrocyte-mediated control of cerebral blood flow. *Nat Neurosci* 9:260–7
- Takata N, Hirase H (2008) Cortical layer 1 and layer 2/3 astrocytes exhibit distinct calcium dynamics *in vivo*. *PLoS One* 3:e2525
- Van Den Pol AN, Romano C, Ghosh P (1995) Metabotropic glutamate receptor mGluR5 subcellular distribution and developmental expression in hypothalamus. *J Comp Neurol* 362:134–50
- Vaucher E, Hamel E (1995) Cholinergic basal forebrain neurons project to cortical microvessels in the rat: electron microscopic study with anterogradely transported *Phaseolus vulgaris* leucoagglutinin and choline acetyltransferase immunocytochemistry. *J Neurosci* 15:7427–41
- Wang XH, Lou NH, Xu QW, Tian GF, Peng WG, Han XN, Kang J, Takano T, Nedergaard M (2006) Astrocytic Ca²⁺ signaling evoked by sensory stimulation *in vivo*. *Nat Neurosci* 9:816–23
- Weber B, Burger C, Biro P, Buck A (2002) A femoral arteriovenous shunt facilitates arterial whole blood sampling in animals. *Eur J Nucl Med Mol Imaging* 29:319–23
- Weber B, Burger C, Wyss MT, von Schulthess GK, Scheffold F, Buck A (2004) Optical imaging of the spatiotemporal dynamics of cerebral blood flow and oxidative metabolism in the rat barrel cortex. *Eur J Neurosci* 20:2664–70
- Winship IR, Plaa N, Murphy TH (2007) Rapid astrocyte calcium signals correlate with neuronal activity and onset of the hemodynamic response *in vivo*. *J Neurosci* 27:6268–72
- Wyss MT, Ametamey SM, Treyer V, Bettio A, Blagoev M, Kessler LJ, Burger C, Weber B, Schmidt M, Gasparini F, Buck A (2007) Quantitative evaluation of ¹¹C-ABP688 as PET ligand for the measurement of the metabotropic glutamate receptor subtype 5 using autoradiographic studies and a beta-scintillator. *Neuroimage* 35:1086–92
- Wyss MT, Obrist NM, Haiss F, Eckert R, Stanley R, Burger C, Buck A, Weber B (2009) A beta-scintillator for surface measurements of radiotracer kinetics in the intact rodent cortex. *Neuroimage* 48:339–47
- Zakharov P, Volker AC, Wyss MT, Haiss F, Calcinaghi N, Zunzunegui C, Buck A, Scheffold F, Weber B (2009) Dynamic laser speckle imaging of cerebral blood flow. *Opt Express* 17:13904–17
- Zonta M, Angulo MC, Gobbo S, Rosengarten B, Hossmann KA, Pozzan T, Carmignoto G (2003) Neuron-to-astrocyte signaling is central to the dynamic control of brain microcirculation. *Nat Neurosci* 6:43–50